Digest Journal of Nanomaterials and Biostructures Vol. 6, No 1, January-March 2010, p. 199 - 206

THE EFFECT OF HYDROGENATION ON THE MAGNETIC PROPERTIES OF LAYERED SPIN VALVE STRUCTURES

V. KUNCSER, F.TOLEA, G.SCHINTEIE, I.JEPU[a], P.PALADE
National Institute of Materials Physics, P.O. Box MG 7, 77125, Bucharest-Magurele, Romania
[a]National Institute for Lasers, Plasma and Radiation Physics, 07712, Bucharest-Magurele, Romania

Multilayer spin valve structures of type AF/F/Cu/F and AF/F/MgO/F (AF=antiferromagnetic layer and F=ferromagnetic layer) have been prepared by sputtering in radiofrequence. The samples were investigated at room temperature by magneto-optic Kerr effect and conversion electron Mössbauer spectroscopy, before and after thermal hydrogenation. Additional magnetic peculiarities were observed at low temperatures via SQUID magnetometry. The effect of the thermal hydrogenation on the magnetic properties of the systems was discussed with respect to the changes in the local spin configuration, observed by Mössbauer spectroscopy.

(Received December 5, 2010; in revised form April 4, 2011; accepted April 6 April 2011)

Keywords: Hydrogen annealing, Multilayers, Mössbauer effect, Magneto-optic Kerr effect, Magnetometry

1. Introduction

A ferromagnetic (F) layer which is interfacially coupled to an antiferromagnetic (AF) layer shows a different magnetization reversal process, as compared to the one of a similar free ferromagnetic layer. In particular, depending on the type of coupling, the magnetic constituents of the F and AF layers and the measurement temperature, the hysteresis loop of the magnetically coupled F/AF bilayer may present a larger coercive field or/and a shift from the zero field. The shift (mainly negative) is known as an exchange bias field, and is related to a so-called unidirectional anisotropy [1], at variance to the coercive field related to an uniaxial anisotropy [2]. Based on the different magnetization reversal processes of the pinned and the free ferromagnetic layers respectively, it can be built a so called multilayer spin valve structure consisting of a nanometer thick conductive layer (or a much thinner isolating layer) interfaced on one side to a pinned F layer and on the other side to a free F layer. The relative spin configuration in the two interfacing F layers can be modified (from parallel to antiparallel) via external magnetic fields. Hence, such multilayer systems can be used as magnetic devices where the electron conduction (or tunneling) is manipulated via Giant Magneto-Resistance (GMR) or Tunneling Magneto-Resistance (TMR) effects [2-3]. The exchange bias field, H_E, of the pinned layer and the coercive field H_C^P (of the pinned layer) and H_C^F (of the free layer) are the main parameters defining the sequential reversal spin behaviour of the structure and hence the electron conduction (tunnelling) in response to the magnetic excitation. They depend on many variables, such as the type of the F films, their crystalline structure and phase composition, the quality of the AF/F interface, etc. [4-6]. In addition, both the exchange bias field and the coercive fields have their own typical decreasing trend versus temperature, due to specific magnetic relaxation mechanisms. With respect to the above mentioned issues, the idea for tuning the magnetic reversal parameters of the spin valve structure via induced structural modifications in the F layers, appears as very interesting. One way to provide such modifications is the thermal hydrogenation of the structure. It has been very

recently proved that at variance to the normal thermal annealing, the thermal hydrogenation might be more effectively, while it combines the structural relaxation induced by annealing with the effect of the structural relaxation induced by hydrogen interstitials [7.8]. This work reports on the effects induced by the thermal hydrogenation on the magnetic reversal behaviour of multilayer spin valve structures of type AF/F/Cu/F and AF/F/MgO/F, providing evidence for a correlation between the change of the magnetic parameters and the change of the local structure in the ferromagnetic layers. One of the most convenient AF materials serving as pinning layer in such spin valve structures is the equiatomic Fe-Mn alloy. Bulk Fe-Mn disordered alloys present the fcc structure (lattice parameter of about 0.36 nm) and antiferromagnetic ordering at room temperature, for Fe concentrations ranging from 45 at. % to 75 at. % [9]. Convenient F layers of low coercivity consist of permalloy and Fe-Co alloys, close to the equiatomic composition. While our interest was to analyse the local structural and magnetic configurations via ^{57}Fe Mössbauer spectroscopy, there have been chosen systems containing the equatomic composition of Fe-Co and Fe-Mn as ferromagnetic and antiferromagnetic layers, respectively.

2. Experimental

The layered structures were grown by radiofrequency (rf) sputtering, excepting the MgO layer which was deposited by thermo-ionic vacuum arc method [6]. It is worth to mention the failure of the rf sputtering method in O_2 atmosphere to provide MgO films of good quality and the capability of the TVA method to provide suitable MgO films of cubic structure (periclase; a=0.422 nm) and of different structural texture, depending on the substrate temperature. In the present case, a substrate temperature of 425 K was used according to previous preparations of thicker MgO films, which X-ray diffraction patterns evidenced just a very intense 200 reflection at 2θ = 42.8 deg. The two prepared samples were (see also Fig.1):

Sample S1 (GMR like spin valve structure with Cu conductive layer): Si (substrate)/Cu(15nm)/$Fe_{50}Mn_{50}$(20nm)/ ^{57}Fe-Co(5nm)/Cu(5nm)/^{nat}Fe-Co(5nm)/Ta(3nm)
Sample S2 (TMR like spin valve structure with MgO isolating layer): Si (substrate)/Cu(15nm)/$Fe_{50}Mn_{50}$(20nm)/ ^{57}Fe-Co(5nm)/MgO(2nm)/^{nat}Fe-Co(5nm)/Ta(3nm)

In the above notation, ^{nat}Fe labels a metallic layer grown from natural Fe (mainly ^{56}Fe and only ~ 2% natural abundance of ^{57}Fe), whereas ^{57}Fe labels a metallic layer 50% enriched in the ^{57}Fe isotope. It is worth mentioning that the crystalline structure and electronic properties of the ^{57}Fe-Co layer are identical to the ^{nat}Fe-Co layer (body centered cubic, bcc), the only difference consisting of the enhanced sensitivity of the tracer layer (almost 25 times higher than for a non-enriched layer of the same thickness) with respect to ^{57}Fe Mössbauer spectroscopy.

The rf sputtering depositions were performed on an one target device, by using a long time (3 hours) base vacuum of $1*10^{-6}$ mbars, before each deposition. The rf discharge was formed in Ar at a pressure of $4*10^{-2}$ mbars, powering the generator at 150 W. The film thickness was controlled via the deposition time (previous calibrations were performed for each film and the overall thickness of the structure was also verified by total interference contrast interferometry). Relative errors of about 10% are expected for the provided thickness, in each case. A commercial $Fe_{50}Mn_{50}$ sputtering target was used for the deposition of the AF films, and a Fe target with Co plackets on top, for the deposition of the ferromagnetic films. In each case, during the deposition of the bottom F film (the one pinned to the AF layer), plackets of metallic Fe, 95% enriched in the ^{57}Fe isotope, were also placed on top of the Fe target, randomly distributed between the Co plackets, leading to a 50% enrichment in ^{57}Fe of the pinned Fe-Co layer. The final multilayer structures, S1 and S2, provided with a Ta cap layer against oxidation, were investigated at room temperature (RT) by longitudinal MOKE (magneto-optic Kerr effect) using laser light of 680 nm. A MOKE device working in longitudinal geometry with possibilities for rotating the sample in its own plane, in order to modify the azimuth between the direction of the magnetic field and an in plane particular direction (e.g. easy axis of magnetization) was used. The employed electromagnet

is provided with laminated sheets with essentially zero remanence and negligible hysteresis. The sample with the most convenient separation of the two loop components was analysed at low temperatures by a SQUID (Quantum Design) magnetometer. The acquisition of the hysteresis loops collected with the field along the sample plane, started from the lowest temperature, after cooling the sample in a magnetic field of 3000 Oe.

The phase composition and local magnetic interactions within the F layer as well as the atomic interdiffusion processes at the interface with the AF layer were investigated by ^{57}Fe conversion electron Mössbauer spectroscopy (CEMS). The CEMS measurements were performed at room temperature with a constant acceleration spectrometer and a gas-flow proportional counter using a He-CH_4 mixture. A ^{57}Co-source in a Rh-matrix was used. All spectra were recorded in perpendicular backscattering geometry, i.e. with the incident γ-ray direction perpendicular to the multilayer plane. The CEMS spectra were fitted using the "NORMOS" package developed by Brand [10]. All isomer shifts (IS) are given relative to bulk α-Fe at room temperature (RT). After taking the above described measurements on the initial samples, these were exposed for 30 minutes to a thermal hydrogenation at 550 K under a hydrogen pressure of 10 bars (previous purging-vacuum steps were applied at 450 K in order to prevent the possible superficial oxidation). The magnetic and Mössbauer characterization were performed also on the new thermally hydrogenated samples, called in the following as S1_h and S2_h.

3. Results and discussion

The MOKE loops obtained on sample S1 and S1_h respectively, at different angles between the applied field and a reference side of the square sample ([110] direction of the Si susbtrate), are shown in Fig.2. At only a glance, it can be observed the in plane magnetic texture of the initial sample which shows an easy axis of magnetization for the both ferromagnetic (pinned and free) layers, along the reference side and a hard axis at 90 deg versus this direction (the squarness of the loops in the first case and the lack of saturation together with the more rounded loop in the second case sustain this affirmation [11]).

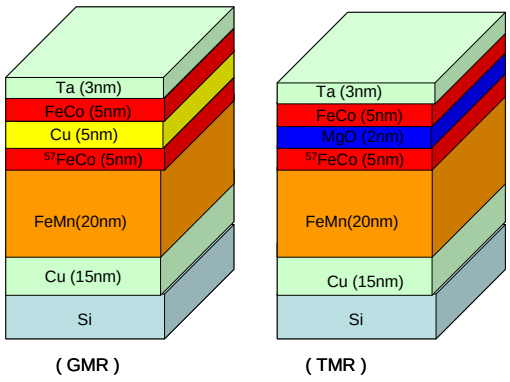

Fig. 1. The geometrical structure of the analyzed systems, namely: S1 (GMR-type with Cu conductive layer) and S2 (TMR-type with MgO isolating layer). In both cases the Fe-Co layer pinned to the AF layer was 50% enriched in the ^{57}Fe isotope.

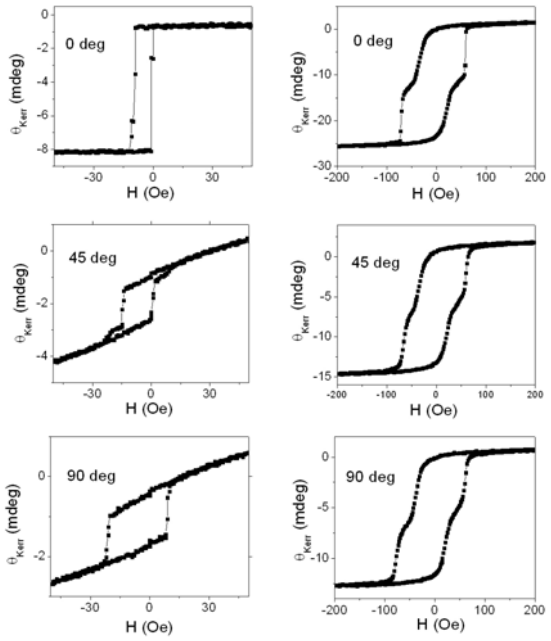

Fig. 2. MOKE loops of samples S1 (left) and S1_h (right) obtained at different angles between the direction of the applied field and a reference side of the square sample ([110] direction of the Si substrate).

On the other hand it may be observed the strong orange-peel coupling between the two F layers in case of a field applied along the easy axis (the two component loops of the structure can be hardly distinguished in this situation) and the much weaker one for a field making 45 deg with this direction (the two components of the complex loop can be well distinguished in this last case). It is worth to mention that the decomposition of the overall complex loop in the constituent loops was analysed in relatively similar systems prepared by molecular beam epitaxy, in reference [12]. Accordingly, to the last case (magnetic field making 45 deg with [110] direction of Si), it can be assigned a coercive field of less than 10 Oe for the free layer and of about 20 Oe, for the pinned F layer (the negative shifts of the loops of 7-10 Oe are assigned to the small remanence of the MOKE magnet). At variance, after the thermal hydrogenation (sample S1_h), the magnetic texture decreases substantially (especially for the pinned F layer) and the coercive field of each ferromagnetic layer becomes almost three times larger (30 Oe for the free layer and 70 Oe for the pinned layer). The separation of the two components of the complex loop becomes more evident and is almost independent on the orientation of the applied field with respect to a peculiar in plane direction. The magnetic antiparallel orientation of the F layers in the thermally hydrogenated samples extends over 40 Oe, as compared with an interval of only 10 Oe in the initial sample.

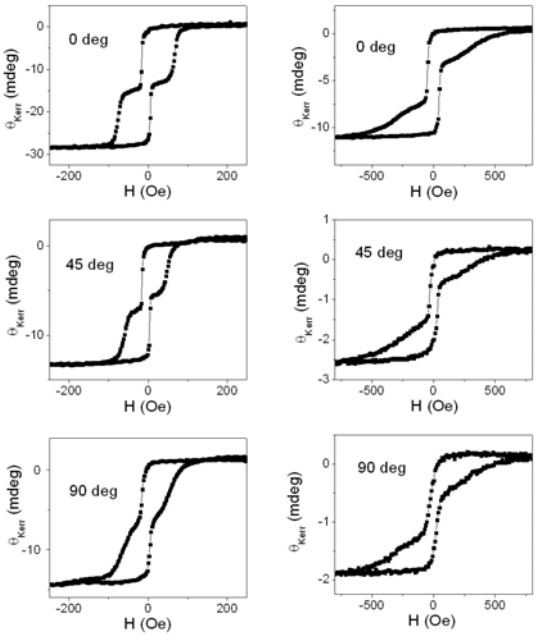

Fig. 3. MOKE loops of samples S2 (left) and S2_h (right) obtained at different angles between the direction of the applied field and a reference side of the square sample ([110] direction of the Si substrate).

The MOKE loops obtained on samples S2 and S2_h, in similar conditions as previously described, are shown in Fig.3. First of all, it should be mentioned the much better delimitation of the two components in the complex loop and the diminished magnetic texture of sample S2 as compared to sample S1. In order to decompose the complex loop in components, we need to decide if mainly an exchange bias field of the pinned layer is involved (so the lower loop is sifted with respect to the upper one) or just different coercive fields, similar to the case of sample S1. The definite response to this issue has arrived only from the magnetization reversal measurements at low temperatures (Fig.4a). It might be clearly observed the negative shift of the loop belonging to the pinned layer (H_E=-150 Oe and H_C=350 Oe) and the negligible exchange bias field and very low coercive field (H_E=0 Oe and H_C=20 Oe) of the loop component belonging to the free F layer. Moreover, the exchange bias field of the pinned layer decreases to zero already at 20 K, giving support for the interpretation of the two components in the complex loop at RT as being related to only different coercive fields of the pinned and free layers, respectively. In this regard, coercive fields of only 10 Oe for the free layer and 90 Oe for the pinned layer are obtained from the RT MOKE loops of sample S2, both of them just slightly dependent on the field orientation. The thermal hydrogenation diminishes again the magnetic texture, especially in the pinned layer and similarly to sample S1_h, increases drastically the coercivity of both ferromagnetic layers (at 30 Oe for the free layer and 280 Oe for the pinned layer). At low temperatures (Fig.4b) the exchange bias field of the pinned layer decreases to zero already at 20 K and the two similar high coercive fields of the loops belonging to the two ferromagnetic layers give rise to just only one common loop which is impossible to be decomposed into components (the two components at RT become visible due to different temperature evolutions of the two coercive fields, almost identical at low temperature).

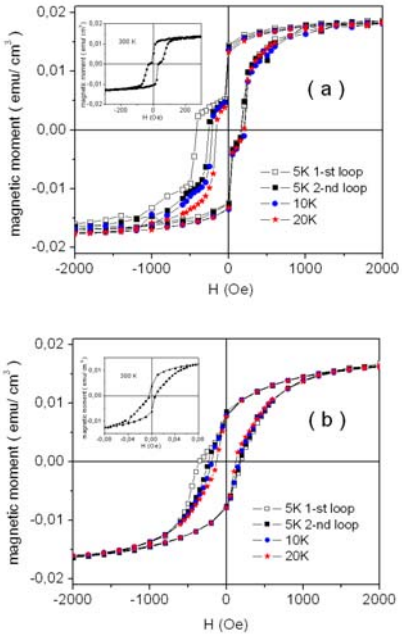

Fig. 4. Low temperature hysteresys loops obtained by SQUID magnetometry on sample S2 (a) and S2_h (b). In insets are shown the loops at 300 K.

The observed magnetic behaviour can be interpreted via additional information provided by Mössbauer spectroscopy.

The ^{57}Fe Mössbauer spectra obtained at RT on all the analysed samples are shown in Fig.5. At a glance, it can be observed the less shaped spectra of the the initial S1 and S2 samples, as compared to the better structured patterns with narrower emission lines, for the thermally hydrogenated samples. Excepting the spectrum of sample S1 which was fitted via a broad sextet (BS) and a central paramagnetic pattern (CP), the best fitting of the rest of spectra was achieved by using three Mössbauer components: (i) a sharp Zeeman sextet (SS), (ii) a broad Zeeman sextet (BS), and (iii) a relatively broad central paramagnetic pattern, taken generally as a doublet (CP). The intensity of the second emission line relative to the third one in each Mossbauer sextet was 4, proving clearly that the Fe spins are aligned in the plane of the F films.

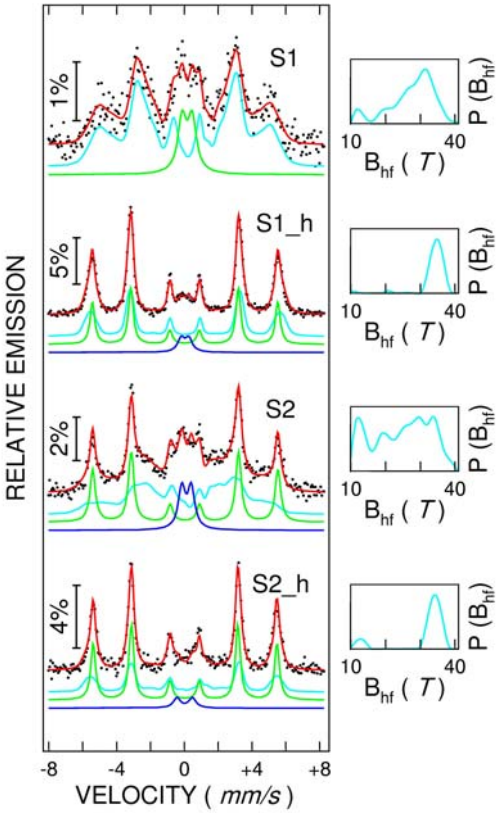

Fig. 5. Room temperature conversion electron Mössbauer spectra of the analysed samples with the pinned layer enriched in the ^{57}Fe. On the right hand are presented the hyperfine field distributions of the broad sextet component of each spectrum.

The BS component was always considered via an hyperfine field distribution, drawn on the right side of each spectrum in Fig.5. The relative spectral area of the BS component and its corresponding hyperfine field distribution is much wider in case of the initial samples as compared to the case of the hydrogenated samples. By the typical hyperfine parameters, the BS component can be related to distributed Fe configurations in the Fe-Co alloy. However, the hyperfine magnetic fields in such alloys can vary only between 0.9 and 1.1 from the value of the hyperfine field in bcc Fe (33.14 T), for the whole range of Co concentrations. Hence, the magnetic hyperfine field of a well structured Fe-Co alloy should take values in the range from 30 T to 36 T. If the distribution probabilities of the BS component in spectra belonging to the hydrogenated samples S1_h and S2_h obey closely this condition, the distribution probability in case of samples S1 and S2 are spread over a much larger interval, taking significant values also for hyperfine fields down to 10 T. Local configurations of the Fe atoms characterized by such low values of the hyperfine fields can be due to either the presence of the nonmagnetic Cu atoms around the central Fe or to an increased topological disorder in the alloy. The first issue is related to a strong atomic interdiffusion at the Fe-Co/Cu interface, which should be already present in the initial samples, whereas the second is related to a structural disorder accompanying the growing process specific to the the rf deposition technique. If the interfacial atomic interdiffusion is in work, the thermal hydrogenation can only activate it, additionally. However, in this case the relative spectral area of the BS component should be even higher in the hydrogenated samples and the hyperfine field distribution should be enlarged, which certainly is not the case. The narrower distribution of hyperfine fields and the lower spectral area of the BS component in the hydrogenated samples seem rather to sustain the effect of the structural relaxation induced by hydrogen interstitials, observed in other class of materials [7,8]. The SS component shows negligible isomer shift and quadrupole splitting (QS) and an hyperfine field of 33.9 T, slightly higher than that of the metallic Fe. It was assigned to the segregation of a certain composition of Fe-Co, strongly enriched in Fe.

The CP component was assigned on base of hyperfine parameters and similar assumptions used in [11] for deriving the expected spectral relative area, to the Fe atoms in the FeMn AF film. In conclusion, the main effect of the thermal hydrogenation is to improve the crystalline structure of the F layer (mainly the pinned layer is observed via the present CEMS measurements) with the formation of a randomly distributed Co-Fe alloy and local partial segregations of an Fe rich composition of the alloy. Hence, the higher coercive fields in the hydrogenated samples are connected to the improved crystalline structure of the F layers induced by their hydrogenation.

4. Conclusions

Multilayer spin valve structures of type Fe-Mn/Fe-Co/Cu/Fe-Co and Fe-Mn/Fe-Co/MgO/Fe-Co were grown by rf sputtering (only the MgO layer was grown by thermo-ionic vacuum arc method in another deposition chamber). The structures have been magnetically characterized (via MOKE, SQUID magnetometry and CEMS) both in the initial state and after a thermal hydrogenation. In a regular way, the hydrogenation increases the coercive field of both the free and the pinned ferromagnetic layer and diminishes the magnetic texture. This behavior seems to be related to an improved polycrystalline structure of the ferromagnetic layers in the hydrogenated samples, induced by a structural relaxation mediated via hydrogen interstitials. Thus, the thermal hydrogenation might be seen as an effective processing procedure for tuning the range of applied fields where the structure is sensitive to the change from parallel to antiparallel magnetic configurations of the ferromagnetic layers.

Acknowledgements

This work was supported by CNCSIS-UEFISCSU, project number PN2-IDEI 1382/2008 of the Romanian Ministry of Education and Research.

References

[1] W. H. Meiklejohn and C. P. Bean, Phys. Rev. **102** , 1413 (1956).
[2] J. Noguès, I. K.Schuller J.Magn.Magn.Mater. **192**, 203 (1999).
[3] M. Johnson, Magnetoelectronics, edited by Elsevier Amsterdam Cap 1 and 2 (2004).
[4] F. Radu, H. Zabel, Exchange Bias Effect of Ferro-/Antiferromagnetic Heterostructures, Springer Tracts in Modern Physics **227**, 97 (2007).
[5] F. Stromberg , W. Keune , V. Kuncser and K. Westerholt, Phys.Rev. B **72**, 064440 (2005).
[6] V. Kuncser, M. Valeanu, G. Schinteie, I. Mustata , C.P.Lungu , A. Anghel , H. Chiriac, R. Vladoiu, J. Bartolome, J.Magn.Magn.Mater. **320**, e226 (2008)
[7] N.Budini, P.A.Rinaldi, J.A.Schmidt, R.D.Arce, R.H.Buitrago, Thin Solid Films **518**, 5349 (2010).
[8] Liu-Niu Tong, Xian-Mei He, Huai-Bin Han Jin-Lian Hu, Ai-Lin Xia and Yan Tong, Solid State Commun. **150**, 1112 (2010).
[9] F. Offi, W. Kuch and J. Kirschner, Phys. Rev. B **66**, 064419 (2002).
[10] R.A., Brand, Nucl. Instr. Meth. Phys. Res. B **28**, 398 (1987).
[11] V. Kuncser, G.Schinteie, P.Palade, I. Jepu, I Mustata, C.P.Lungu, F.Miculescu and G.Filoti, Journal of Alloys and Comp. (2010)
[12] V. Kuncser, W.Keune, U. von Hörsten, G.Schinteie, J. Optoelectron. Adv. Mater. (2010)
[13] V. Kuncser, W.Keune, U. von Hörsten, G.Schinteie, N.Stefan, P.Palade, G. Filoti, Thin Solid Films, **518**, 5981 (2010)